

StreamOptix: A Cross-layer Adaptive Video Delivery Scheme

Mufan Liu, *Student Member, IEEE*, Le Yang, *Member, IEEE*, Yifan Wang, Yiling Xu, *Member, IEEE*, Ye-Kui Wang, Yunfeng Guan

Abstract—This paper presents a cross-layer video delivery scheme, StreamOptix, and proposes a joint optimization algorithm for video delivery that leverages the characteristics of the physical (PHY), medium access control (MAC), and application (APP) layers. Most existing methods for optimizing video transmission over different layers were developed individually. Realizing a cross-layer design has always been a significant challenge, mainly due to the complex interactions and mismatches in timescales between layers, as well as the presence of distinct objectives in different layers. To address these complications, we take a divide-and-conquer approach and break down the formulated cross-layer optimization problem for video delivery into three sub-problems. We then propose a three-stage closed-loop optimization framework, which consists of 1) an adaptive bitrate (ABR) strategy based on the link capacity information from PHY, 2) a video-aware resource allocation scheme accounting for the APP bitrate constraint, and 3) a link adaptation technique utilizing the soft acknowledgment feedback (soft-ACK). The proposed framework also supports the collections of the distorted bitstreams transmitted across the link. This allows a more reasonable assessment of video quality compared to many existing ABR methods that simply neglect the distortions occurring in the PHY layer. Experiments conducted under various network settings demonstrate the effectiveness and superiority of the new cross-layer optimization strategy. A byproduct of this study is the development of more comprehensive performance metrics on video delivery, which lays down the foundation for extending our system to multimodal communications in the future. Code for reproducing the experimental results is available at <https://github.com/Evan-sudo/StreamOptix>.

Index Terms—Cross-layer design, adaptive bitrate, video delivery, link adaptation, resource allocation.

I. INTRODUCTION

The deployment of 5G technology promotes the rapid proliferation of mobile video streaming. According to Ericsson’s annual report 2022 [2], it is anticipated that the volume of mobile data traffic will double between 2023 and 2027, with an annual growth rate of nearly 30%. On the other hand, this poses significant challenges to the development of efficient methods for video delivery, due to the increase in the complexity of wireless transmission scenarios and higher user expectations for viewing experiences.

To attain satisfactory quality of experience (QoE) in a fast-changing environment, methods for optimizing video delivery have been proposed. Among them, more than half were built on Dynamic Adaptive Video Streaming over HTTP (DASH) [3], which serves as the backbone for realizing various video delivery strategies in the last decade. In DASH, videos are

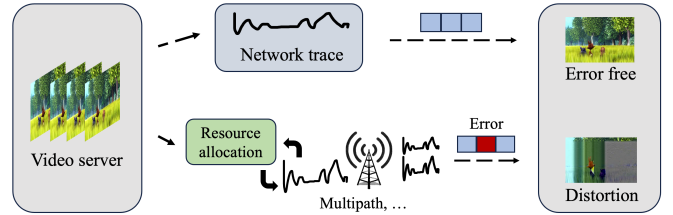


Fig. 1: Trace-driven ABR environment (upper) overlooks the effect of resource allocation and channel fading over wireless link (bottom).

first segmented and encoded into chunks with different bitrates and resolutions, more commonly known as representations, and are then stored on the server. When the video content is requested, the DASH server considers both playback and network conditions such as buffer size and throughput¹, and switches among the available chunk representations to ensure good QoE. This process, referred to as the adaptive bitrate (ABR), enables the system to adapt to the fluctuating network conditions and guarantees a seamless playback experience. In real world, video transmission encompasses not just the upper-layer ABR but also the complex lower-layer wireless link, commonly referred to as the ‘last mile’ transmission [4]. The large gap between these two layers has led to previous studies on video delivery treating them separately. This separation has resulted in an optimization bottleneck in current video delivery research.

A. Motivation

ABRs are currently evaluated in a way at the application layer (APP) without any transmission error, known as trace-driven simulation. This method simulates video streaming by using precollected throughput traces. It updates the video downloading and playback processes effectively based on the correlation between the video size and throughput trace. However, trace-driven environment overlooks the impact of the wireless link, despite its simplicity and speed. As a result, real world video streaming entails intricate wireless link transmissions, leading to distortions caused by multipath fading and fluctuations in throughput due to resource allocation. (Fig. 1). To emphasize its effects, we constructed a 5G physical downlink shared channel (PDSCH) to test existing DASH-based ABRs and analyzed the decoded bitstreams².

¹Throughout this paper, we say **throughput** when talking about network bandwidth and **bitrate** when talking about encoding quality.

²The experimental setup was based on the static configuration described in Section 4, but retained the default settings for link adaptation and resource allocation.

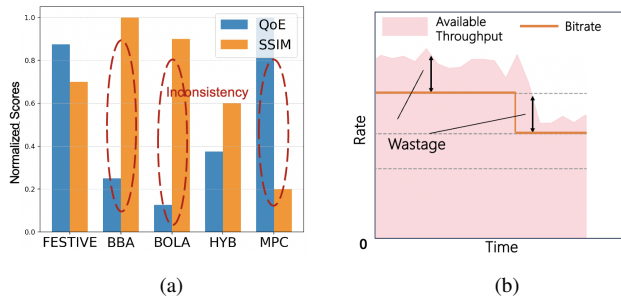


Fig. 2: Evaluation of existing ABR strategies under simulated 5G wireless links. (a) Inconsistency between the predicted QoE and actually received SSIM. (b) Gap between the selected video bitrate and link capacity.

As depicted in Fig. 1, resource allocation modifies throughput during streaming, which is unobservable in a trace-driven environment. Subsequently, the video displays arbitrary distortions following the fading of the wireless link. To sum up, the evaluation revealed two issues. First, Fig. 2a shows that **higher QoE scores, estimated by ABRs based on the selected bitrates, do not always correspond to better received visual quality** (in this experiment, the structural similarity (SSIM) quality metric was used). In other words, there exists *inconsistency* between the ABR-predicted QoE and actually received visual quality scores post wireless transmission. Neglecting the transmission errors in this case leads to overestimated user QoE by ABRs.

Another observation is illustrated in Fig. 2b. We noticed an **evident gap between the selected bitrates and instantaneous network capacity**. Due to the inherently ill-posed nature of throughput prediction, it is inevitable that the video bitrate based on predicted throughput will deviate from the actual throughput (see e.g. [5]–[8]). Improved throughput prediction algorithms were proposed in [9], [10], but they did not utilize that the throughput can in fact be recontrolled after prediction. In fact, incorporating video bitrate considerations into resource allocation to control throughput can effectively reduce this gap.

Traditionally, link control conducted at PHY and MAC was decoupled from the APP, focusing on optimizing the Quality of Service (QoS) of the network only while ignoring the video-aware information [4], [11]–[14]. Besides, the ABR mechanisms in APP usually lack the use of feedbacks from the PHY and MAC layers, resulting in inaccurate evaluation of the QoE, as well as limited performance gain. Existing cross-layer studies either followed a top-down or bottom-up approach in their designs [4], [11], [14]–[16]. However, the complex interplay between layers was not fully exploited, and a closed-loop cross-layer technique is yet to be developed. Moreover, these work did not construct and provide a practical and efficient cross-layer video delivery platform. These motivate taking a cross-layer approach that integrates ABR with link adaptation in PHY and resource allocation in MAC to combat link distortions and improve bitrate utilization jointly.

B. Our design

This paper presents a three-level closed-loop cross-layer framework for optimizing video delivery. Our method integrates the PHY, MAC, and APP layers. In the APP, we employ model predictive control (MPC) for rate adaptation

based on the link capacities provided by PHY. The throughput measured in APP is no longer used, because it is an irregularly sampled sequence (ISS) due to the fluctuations in the chunk downloading time. In contrast, the intervals for estimating the link capacities at PHY are much smaller [4], which ensures a sequence of a uniformly spaced measurement samples. The selected bitrate at APP is that passed down to MAC in order to perform the video-aware resource allocation, aiming to maximize throughput utilization. Meanwhile, the allocated resource blocks (RB) count is transmitted to PHY as well, which is combined with a newly proposed soft link adaptation scheme there to decrease the error rate and improve the stability of throughput. The entire optimization process forms a closed loop, and the effectiveness of our proposed system was proved through extensive evaluations.

Our contributions include

- We construct the cross-layer video transmission platform, which encompasses the PHY, MAC, and APP layers. It can accurately emulate both the link transmission and playback of video delivery.
- We designed a three-level closed-loop cross-layer video delivery framework. This scheme effectively addresses the optimization needs of different layers. It also achieves cross-layer interaction and cooperative optimization.
- Extensive evaluations were conducted and we collected the distorted video streaming for further objective quality assessment to highlight the gains brought by our cross-layer design.

The rest of this paper is organized as follows. Sec. I A. provides an overview of related work. Sec. II formulates the cross-layer QoE maximization problem in consideration. In Sec. III, we present the design of the cross-layer framework and Sec. IV gives the evaluation results. Finally, the paper is concluded in Sec. V.

C. Related work

Video delivery across different layers: Studies on video delivery are carried out in the PHY, MAC, transport, and APP layers of the communication network. Each layer employs distinct strategies and metrics for adaptive control. In the PHY layer, link adaptation is the process of adaptively selecting modulation and channel coding rate (MCS) guided by channel feedback to enhance channel throughput and minimize transmission errors. The default 3GPP [17] method of link adaptation, known as inner loop link control (ILLA), employs a pre-established SNR-MCS lookup table to determine the choice of MCS based on real-time SNR estimates. To cope with SNR variations and delays, outer loop link adaptation (OLLA) is proposed by adding an extra offset to the SNR estimate, which is adjusted according to positive/negative acknowledgements (ACK/NACKs) received in the past transmissions [18]. More recently, [19]–[21] employ either a rule-based or learning-based strategy for MCS adaptation based on multi-dimensional channel states, rather than just the SNR, to further boost the performance of link adaptation. However, the impact of link adaptation on throughput is localized as it only affects the size of each individual RB. [22] further requires resource

allocation at MAC to make fine adjustments to the number of RBs. Existing resource allocation schemes are either based on proportional fairness or round-robin strategy [1], [23], which achieves equitable distribution by minimizing differences in resource allocated to different users. They largely ignore the video information from the APP layer.

The APP layer has consistently been a focus in video delivery, primarily because it enables macro-level control over video quality and bitrate. Based on the architecture of traditional HTTP adaptive streaming, a collection of ABR approaches have been proposed to ameliorate user's QoE. They can be classified as heuristic-based and learning-based. Heuristic-based ABRs [5], [6], [8], [24], [25] establish predefined rules that consider buffer status, estimated throughput, or both, to determine bitrate, providing a straightforward and effective solution. For instance, FESTIVE [8] predicts the future chunk throughput based on history measurements and selects the video bitrate that is closest to the predicted throughput. Since accurate throughput prediction is hard in reality, buffer-based ABRs [5], [26] avoid direct throughput measurement by choosing the bitrate based on the playback buffer occupancy. To achieve a good trade-off between rate and buffer goals, MPC [6] employs a hybrid strategy which first forecasts future chunk throughput using past data and solves the optimization problem for delivering upcoming chunks by integrating both bitrate and buffer considerations. On the other hand, learning-based ABRs [7], [27], [28] utilize advanced deep learning techniques, making the derived methods applicable to a wider variety of situations. Pensieve [7] employs deep reinforcement learning (DRL)-based framework for ABR by optimizing the QoE function defined in [6].

Although these studies have established remarkable control mechanisms, they lack integration of and interaction across different layers. This has motivated the study of optimization strategies that span multiple layers.

Cross-layer designs: As the bitrate decisions at APP form the foundation for video delivery, most cross-layer optimization methods in video delivery involve the integration of APP with other lower layers [29], [30]. In the following, we'll review cross-layer designs that merge APP with the wireless link. This consists of two aspects: integrating ABR at APP with MAC and PHY.

Current cross-layer work with MAC adds the constraint of limited resources within the adaptive streaming process, thereby achieving optimized resource allocation. For instance, [23] introduces an DRL-based resource allocation strategy to tradeoff QoE fairness among different users. [31] proposes a pseudo-polynomial time optimal algorithm to adaptively adjust video encoding configuration under given resource constraint. [32] jointly optimizes the multi-user access and video bitrate under a large number of users associated with limited transmission time slots. Meanwhile, [33] deploys a multi-step Deep Q-network for frame-priority-based wireless resource scheduling and a transformer-based proximal policy optimization (TPPO) for video bitrate adaptation. [34] proposes an adaptive GoP-level FEC allocation strategy based on the video slice header information. But it does not include the adaptation for video bitrate. Nonetheless, these MAC-APP cross-layer designs ei-

ther consider bitrate adaptation under limited resources or re-design resource allocation given a fixed APP information. Given the complexity of channel variations, PHY is often referred to as "the last mile transmission", showing their significant impact on video delivery. Consequently, many studies have been devoted to optimizing the video delivery with the PHY layer information. [35] enables continuous monitoring of the LTE base station's cellular data to estimate the throughput, which is used to optimize throughput prediction in the APP layer. Similarly, [12]–[14], [36] considers video delivery on the physical downlink shared channel (PDSCH) and makes bitrate decisions based on link throughput measurement. [16] explores adaptive video delivery for multiple users across a time-varying and mutually interfering multi-cell wireless network. They consider the impact of the video content complexity on resource allocation and conducts offline training of the ABR agent based on PHY network throughput traces. [34] dynamically selects the MCS for video block transmission under given video source to maximize user experience. Cross-layer designs integrating PHY and APP face similar problems as those combining MAC. For instance, in [16], they first collect network traces under their proposed resource allocation scheme and then use the collected trace for offline training of the ABR agent. The lack of interaction between layers in existing cross-layer methods highlights the need for a more comprehensive evaluation platform for cross-layer designs in video delivery.

II. CROSS-LAYER QOE MAXIMIZATION

A. Framework

We consider the single-user 5G video delivery scenario shown in Fig. 3, as the multi-user case inevitably involves a tradeoff between the fairness and each user's QoE. Later, we are going to show how our cross-layer design can be extended to the scenario with multiple users.

The system includes a DASH server and a user equipment (UE). It has three layers, PHY, MAC and APP. At APP, the server stores several video files, each is divided into smaller chunks of T_{chunk} seconds. Without loss of generality, we assume there are one video file consists of D chunks, indexed as $\{1, 2, \dots, D\}$. Each video chunk is encoded into L different representations (i.e., quality levels), with $a_{i,l}$ ($i = 1, 2, \dots, D; l \in \{1, 2, \dots, L\}$) denoting the l -th bitrate for chunk i . The available representations for each video chunk are specified in the Media Presentation Description (MPD) file, which is periodically updated. DASH users can access the MPD file by sending an HTTP request. Upon requesting the download of a new chunk, the requested chunk is delivered over the 5G PDSCH. The throughput of this link is jointly affected by the allocation of RBs at MAC and the MCS at PHY. Prior to a new download request, UE needs to make the bitrate decision for the chunk to be delivered next, based on link throughput and playback information.

B. Wireless Link

We consider a single-link multipath channel with slow block fading. The channel impulse response remains stationary

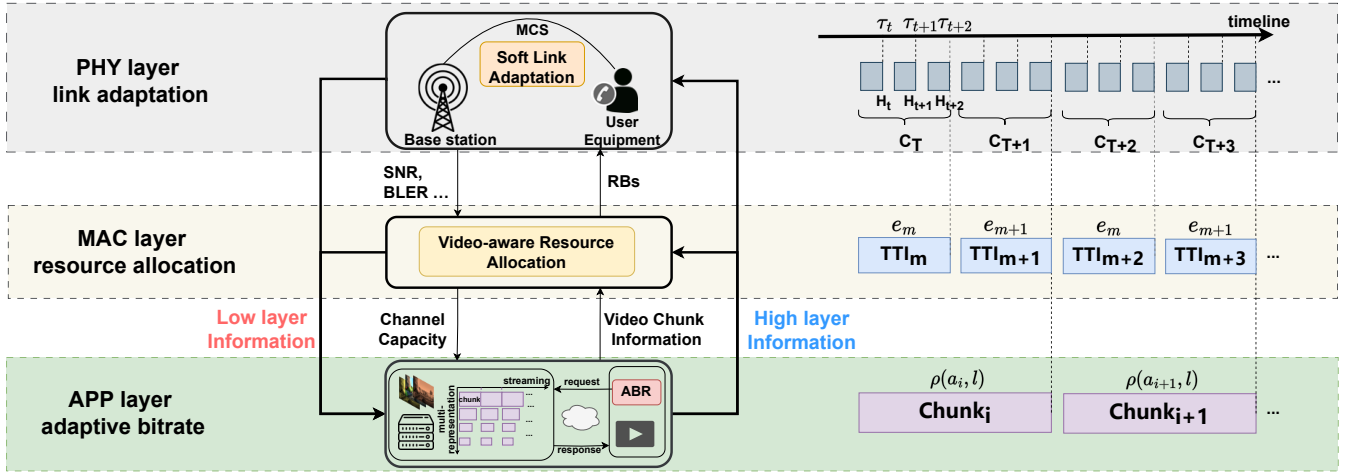


Fig. 3: A schematic diagram of the cross-layer adaptive video delivery system.

during one time slot [37]. For time slot t , the user sends one transport block (TB) of several OFDM symbols, which are collected in the columns of \mathbf{x}_t . Assuming a time-varying but linear channel model with channel coefficient matrix \mathbf{H}_t , normalized symbols and additive Gaussian noise \mathbf{n}_t . we can write the received TB at the UE as

$$\mathbf{y}_t = \mathbf{H}_t \mathbf{x}_t + \mathbf{n}_t. \quad (1)$$

With the 5G PDSCH, data streams from upper layers are encapsulated into separate TBs for "the last mile transmission". Each TB is composed of several RBs, and RB is the smallest allocation unit in the time-frequency domain. The scheduler in MAC determines the number of RBs at each transmission time interval (TTI), typically at intervals that are multiples of the time slots (i.e. 1 TTI = m time slots). The number of allocated RBs e_t at time slot t must satisfy

$$0 \leq e_t \leq e_{max}, \quad (2)$$

where e_{max} is the total number of available RBs. Clearly, the number and size of allocated RBs directly affects the size of the TB. In particular, the size of each TB is determined by the MCS. MCS is selected by the base station at each time slot based on signal-to-noise ratio (SNR) estimation from a UE. As specified in [17], every MCS is associated with a SNR range in a lookup table ($\mathcal{T} = \{\tau_1, \tau_2, \dots, \tau_T\}$).

We use the exponential effective SNR mapping (EESM) [38] to calculate the SNR γ_t of a TB as

$$\gamma_t = \beta \ln \left(\frac{1}{N} \sum_{k=1}^N \exp \left(\frac{\|\hat{\mathbf{h}}_k\|^2 / (y_{t,k} - \hat{\mathbf{h}}_{t,k}^T \mathbf{x}_t)^2}{\beta} \right) \right), \quad (3)$$

where $y_{t,k}$ is the k -th element in \mathbf{y}_t . $\hat{\mathbf{h}}_{t,k}^T$ is the k -th row of $\hat{\mathbf{H}}_t$, which is the estimated channel state information (CSI) and can be acquired via channel estimation. β is a tuning parameter.

We employ a probabilistic formulation to model the link adaptation strategy. Specifically, let $p_{\tau,\gamma}$ be the joint density that indicates the probability of choosing MCS τ at SNR γ . In

order to ensure reliable transmission, it is essential to impose the constraint

$$\sum_{\tau} \int_{\gamma} p_{\tau,\gamma} \eta_{\tau,\gamma} d\gamma \leq \eta_0. \quad (4)$$

The block error rate (BLER) $\eta_{\tau,\gamma}$ is the likelihood of incorrectly decoding TB with MCS τ at SNR γ . Eq. (4) states that the average BLER of the system is expected to be below a predefined threshold η_0 . Surpassing this threshold means an increase in the video packet error rate, causing decoding issues. The TB needs to be re-transmitted as long as its decoding is incorrect, thereby leading to increased transmission delay. The default link adaptation strategy is to directly select a MCS using the deterministic MCS lookup table, according to the SNR estimate. The wireless link also employs the hybrid automatic repeat request (HARQ) mechanism, which sends ACK or NACK signals to show whether each TB has been received successfully.

C. Video playback

We consider a situation where a user requests to watch a video file and downloads video chunks of the specified representations sequentially. Recall that $a_{i,l}$ is the bitrate chosen for the i -th chunk at l -th representation. Suppose at time t_i , the user initiates the downloading of video chunk i . We assume that the player will request the next chunk immediately after receiving the current one. That is, $t_{i+1} = t_i + d_i$, with d_i denoting the downloading time for chunk i . Let $\rho(a_{i,l})$ be the chunk size under chunk representation $a_{i,l}$. The downloading time d_i would be $d_i = \rho(a_{i,l})/C_i$, where C_i is the network throughput during the download process. C_i can be found by computing the mean of the instantaneous transmission rates across all time slots while chunk i is being downloaded as

$$C_i = \frac{1}{t_{i+1} - t_i} \sum_{t=t_i}^{t_{i+1}} \frac{N_{\tau_t, e_t}}{\Delta T_{\text{slot}}} (1 - \eta_{\tau_t, \gamma_t}). \quad (5)$$

N_{τ_t, e_t} is the TB size under MCS τ_t and RB number e_t . ΔT_{slot} is the duration for each time slot. The rightmost term of Eq. (5) is actually the inverse of the average number of transmissions

TABLE I: Nomenclature.

Symbol	Description	Symbol	Description
Video playback notations			
$\mathcal{D} = \{1, 2, \dots, D\}$	The set of D video streams.	$\{1, 2, \dots, D\}$	The set of video chunks in a video file.
ϕ_i	The rebuffering time for chunk i	T_{chunk}	The duration of a video chunk.
C_i	The average throughput at chunk i .	b_i	The buffer size at chunk i .
t_i	The time to start downloading chunk i .	d_i	The download time for chunk i .
$a_{i,l} \in \mathcal{A}_D$	The bitrate of i -th chunk, l -th representation.	$\rho(a_{i,l})$	The size of i -th chunk, l -th representation.
Link notations			
$\mathbf{X}_t = [1_t, 2_t, \dots, x_t]$	The sequence of transmitted symbols.	Φ	The threshold for discriminating soft-ACK.
$\mathbf{Y}_t = [1_t, 2_t, \dots, y_t]$	The sequence of received symbols of \mathbf{X}_t .	$\mathbf{H}_t = [1_t, 2_t, \dots, h_t]$	The sequence of CSI.
$\mathcal{T} = \{\tau_1, \tau_2, \dots, \tau_T\}$	The set of all available MCSs defined in 3GPP.	e_t	The allocated RB count at t .
N_{τ_t, e_t}	The size of TB assigned with τ_t and e_t .	γ_t	The measured channel SNR.
$p_{\tau, \gamma}$	The BLER under MCS τ and SNR γ .		
η_{γ_t, τ_t}	The BLER under SNR γ_t and MCS τ_t .	ΔT_{slot}	The length of a time slot in seconds.
δ_t	The OLLA offset at time t .	$\Delta_{\text{down}}, \Delta_{\text{up}}$	Outer loop link adaptation deviation parameters.

required for a successful chunk decoding. In practice, we do not know the exact value of η_{τ_t, γ_t} and it is replaced by the proportion of retransmissions during the chunk delivery. The network throughput C_i is upper-bounded by the Shannon's capacity [39] as

$$C_i \leq \frac{1}{t_{i+1} - t_i} \sum_{t=t_i}^{t_{i+1}} e_t \cdot \log_2 \left(1 + \frac{\gamma_t}{e_t} \right). \quad (6)$$

The received video chunks are stored in the user playback buffer. The buffer occupancy when the user starts downloading chunk i is denoted as $b_i \in [0, b_{\max}]$. Rebuffering would occur when the buffer is depleted, indicating that the download time d_i exceeds the buffer level b_i . Rebuffering time ϕ_i can thus be expressed as

$$\phi_i = (d_i - b_i)_+ = \left(\frac{\rho(a_{i,l})}{C_i} - b_i \right)_+, \quad (7)$$

where $(x)_+ = \max\{x, 0\}$. We can write the evolution of the playback buffer occupancy as

$$b_{i+1} = (b_i - d_i) + T_{\text{chunk}}. \quad (8)$$

D. Problem Formulation

To ensure a smooth playback, frequent quality variations and rebuffering events should be minimized while maximizing the bitrates of transmitted videos. We define the reward for measuring user QoE [6] as

$$\text{QoE}_i = a_{i,l} - \alpha |a_{i,l} - a_{i-1,l}| - \beta \phi_i, \quad (9)$$

where α and β are non-negative parameters used to adjust the importance of quality fluctuations and rebuffering events in the QoE evaluation.

With the user mobility and channel fading, the wireless channel conditions between base stations and mobile users vary over time. In contrast, watching a video clip typically takes a relatively longer time. To ensure a high QoE for the user over this extended period, we formulate the overall QoE optimization for video delivery as

$$\mathbf{P1:} \quad \max_{\tau, e, a} \sum_{i=1}^D \text{QoE}_i$$

s.t. Constraints from Eqs. (1), (2), (4), (6), (7), and (8).

Decision variables for this problem are 1) MCSs at PHY: $\tau = \{\tau_t\}_{t=1,2,\dots}$, adjusted every time slot; 2) number of RBs at MAC $e = \{e_t\}_{t=m,2m,\dots}$, adjusted every TTI and 3) video bitrate at APP $a = \{a_{i,l}\}_{i=1,2,\dots,D; l \in \{1,\dots,L\}}$, adjusted every chunk. This is a NP-hard problem and involves three decision spaces with varying timescales. To simplify the above cross-layer optimization problem, we decompose the it into three parts, namely (PHY) link adaptation, (MAC) resource allocation and (APP) bitrate adaptation.

III. DESIGN OF STREAMOPTIX

A. System Overview

With the proposed StreamOptix system, at the PHY layer, channel capacities are measured uniformly in time to produce the regularly sampled sequence (RSS). The RSS is input to APP to determine the chunk bitrate using MPC. The optimal bitrate that maximizes the future chunks' QoE is found. The selected bitrate is then sent to lower layers to guide the wireless link control. Specifically, MAC allocates resource to maximize the rate utilization given the target video bitrate. The selected RB number is forwarded to PHY to constrain the link adaptation at smaller timescales and minimize the transmission errors. During the link adaptation process, PHY keeps gathering CSI to obtain link capacity measurements, which are sent to APP for future bitrate decisions. Our design thus leads to the establishment of a closed-loop control system whose modules (i.e., layers) operate at different timescales.

B. PHY: Soft Link Adaptation

According to Eq. (5), the system throughput is limited by the link BLER in the sense that a large BLER could cause an increased number of retransmissions. In this case, transmitting high-bitrate videos may not improve the user QoE, as it could result in frequent rebuffering (see Eq. (7) and (Eq. 9)).

To improve the quality of video delivery and achieve more robust link performance, an efficient link adaptation scheme is developed to cope with changing network conditions. In contrast to the chunk-level decisions made at APP, link adaptation aims at inducing macroscopic changes through small-scale adjustments. Hence, when designing link adaptation schemes, it is essential to take into account our targets (i.e. throughput or BLER) in terms of their average values.

In order to maintain a low BLER while transmitting high-quality video, we formulate the link adaptation problem as

$$\mathbf{P2:} \quad \max_{\{\tau_t\}_{t=1,2,\dots}} \sum_t N_{\tau_t, e_t} (1 - \eta_{\gamma_t, e_t})$$

s.t. Constraints from Eqs. (1), (3), (4), and (6).

The default 3GPP method of link adaptation employs the MCS lookup table to determine MCS based on SNR estimates. The MCS lookup table [17], generated by 3GPP through offline simulations under various link conditions, identifies the MCS that maximizes throughput at different SNR levels. Nevertheless, the actual link often exhibits complex variations that prevent achieving the desired BLER performance using this table alone. To address this issue, OLLA was designed to dynamically incorporate an offset related to HARQ feedback into the estimated SNR, aiming to mitigate excessive BLER. While this method does lower BLER, it exhibits slow convergence. Therefore, we integrate a novel mechanism called soft-ACK with OLLA to further enhance its BLER convergence and efficacy.

OLLA: In the default link adaptation mode specified by 3GPP, the base station (BS) computes the SNR based on the CSI estimation at each time slot and subsequently chooses the MCS according to a predefined lookup table. However, the MCS decisions could be prone to inaccuracies due to channel fluctuations and CSI reporting delays. These lead to suboptimal performance and may not ensure fast BLER convergence. In order to address this weakness, OLLA is proposed to handle SNR inaccuracies by modifying the measured SNR values from the CSI report using an estimated offset δ_t before linking them to the MCS index. Specifically, OLLA fine-tunes the SNR estimate using

$$\hat{\gamma}_t = \gamma_t - \delta_t. \quad (10)$$

Based on the HARQ feedback, the offset δ_t is updated as

$$\delta_t = \begin{cases} \delta_{t-1} + \Delta_{\text{up}}, & \text{if NACK} \\ \delta_{t-1} - \Delta_{\text{down}}, & \text{if ACK.} \end{cases} \quad (11)$$

Each $(\Delta_{\text{up}}, \Delta_{\text{down}})$ pair corresponds to different BLER convergences and is set according to the specific requirement and link conditions. When the UE HARQ feedback is NACK, the offset is incremented; conversely, it is decremented.

In the following, the convergence of the OLLA algorithm under stationary link conditions, as well as the conditions that Δ_{down} and Δ_{up} should be satisfied in order to achieve convergence, is studied.

Theorem 1. *The BLER of OLLA will converge to $\frac{1}{1 + \frac{\Delta_{\text{up}}}{\Delta_{\text{down}}}}$ if $\Delta_{\text{down}} + \Delta_{\text{up}} < \frac{2e}{1.11}$.*

Proof. Let $I(\cdot)$ denote the indicator function. We can rewrite (10) and (11) as

$$\delta_t = \delta_{t-1} + I(\text{NACK})\Delta_{\text{up}} - I(\text{ACK})\Delta_{\text{down}}. \quad (12)$$

Taking expectation on both sides of (12) yields the recurrence function for δ , which is

$$T(\delta) = \delta + \eta_t \Delta_{\text{up}} - (1 - \eta_t) \Delta_{\text{down}}, \quad (13)$$

where η_t is the average BLER at time t .

According to [37], for a random sequence to converge, its recurrence function must satisfy both the first and second Banach fixed point conditions. The first Banach fixed point condition states that the recurrence function should be a contract mapping. That is, we require that

$$T(\delta) \in [\delta_{\min}, \delta_{\max}], \forall \delta \in [\delta_{\min}, \delta_{\max}]. \quad (14)$$

Firstly, the values of η_t are between 0 and 1. With the continuing reception of ACKs, there exists a sufficiently small $\delta_t = \delta_{\min}$ such that an overestimate of the SNR is obtained, thereby yielding eventually $\eta_t = 1$ and an NACK being received. In this case, we have $T(\delta_{\min}) = \delta_{\min} + \Delta_{\text{up}}$. Next, as δ_t increases, the value of η_t starts to decrease until δ_t reaches a value δ_{\max} high enough to ensure that the SNR is underestimated and $\eta_t = 0$. In this case, we obtain $T(\delta_{\max}) = \delta_{\max} - \Delta_{\text{down}}$. In summary, it can be concluded that

$$T(\delta) \in [\delta_{\min} + \Delta_{\text{up}}, \delta_{\max} - \Delta_{\text{down}}] \in [\delta_{\min}, \delta_{\max}], \forall \delta \in [\delta_{\min}, \delta_{\max}]. \quad (15)$$

The second Banach fixed point condition states that

$$|T'(\delta)| < 1, \forall \delta \in [\delta_{\min}, \delta_{\max}]. \quad (16)$$

The proof for the second Banach fixed point condition is included in Appendix A.

As a result, according to the Banach fixed-point theorem [40], when t approaches infinity, the recurrence equation in (13) converges to the unique solution, which is obtained through setting $T(\delta) = \delta$,

$$\lim_{t \rightarrow \infty} \eta_t = \frac{1}{1 + \frac{\Delta_{\text{up}}}{\Delta_{\text{down}}}}. \quad (17)$$

□

By accumulating the small adjustments triggered by ACKs and NACKs over time, OLLA eliminates the discrepancy between the target BLER and the estimated BLER. The offset δ_t will finally reach a steady state when the system converges to the BLER target.

Soft Link Adaptation: Empirically, Δ_{down} is set to be a small value for OLLA to achieve the BLER target. However, this could result in a lengthy convergence period much longer than the duration of a chunk. Moreover, depending solely on OLLA for offset adjustments may not enable quick discovery of poor channel conditions, since OLLA reduces the SNR estimate only after receiving a NACK. Meanwhile, the network conditions may have deteriorated significantly. Therefore, it is crucial to develop an approach that achieves faster convergence and lower BLER. For this purpose, we redefine the ACK levels, making them dependent on the channel's metrics (i.e., BLER). This is referred to as soft-ACK. Soft-ACK divides the prediction intervals of a specific channel metric to categorize various ACK levels [41]. It captures more channel information by increasing the ACK granularity, thus attaining higher sensitivity to channel degradation.

We introduce two levels of ACKs: high-margin-ACK and low-margin-ACK. High-margin-ACK is treated as a "good" ACK which triggers a decrease by Δ_{down} to the SNR offset

δ_t . On the other hand, a low-margin-ACK is considered as a NACK, leading to an increase in the offset by Δ_{up} . The distinction between high- and low-margin ACKs is made using the BLER threshold Φ [42]. If the BLER is below this threshold Φ , it indicates an effective ACK (High-margin-ACK). If not, the ACK is categorized as low margin, indicating a potential channel quality degradation. Given that the BLER for each TB is not directly available, we utilize an empirical equation to approximate the BLER $\hat{\eta}_{\tau_t, \gamma_t}$ at t . This approximation is reliant on the estimated SNR and the MCS, which is [43]

$$\hat{\eta}_{\tau_t, \gamma_t} = 1 - \frac{1}{2} \left(1 + \operatorname{erf} \left(\frac{\gamma_t - \gamma[\tau_t] + \alpha}{\sqrt{2}} \right) \right). \quad (18)$$

Here, γ_t is the estimated SNR at t , τ is the selected MCS. $\gamma[\tau_t]$ is the SNR threshold of MCS τ_t defined in [17] and α is a tunable parameter.

The convergence of soft-ACK under stationary link conditions, as well as the conditions that should be satisfied is studied in the following.

Theorem 2. *The BLER of soft link adaptation will converge to a target that is smaller than $\frac{1}{1 + \frac{\Delta_{\text{up}}}{\Delta_{\text{down}}}}$ if the following conditions are hold:*

- The threshold Φ for determining low-margin-ACKs is greater than or equal to $\frac{1}{1 + \frac{\Delta_{\text{down}}}{\Delta_{\text{up}}}}$.
- $\Delta_{\text{up}} < \frac{2e}{1.11}$.

Proof. We can write the transition for δ_t under soft link adaptation as

$$\begin{aligned} \delta_t = & \delta_{t-1} + \text{I(NACK)}\Delta_{\text{up}} - \text{I(ACK)} \Pr(\hat{\eta} \leq \Phi)\Delta_{\text{down}} \\ & + \text{I(ACK)} \Pr(\hat{\eta} > \Phi)\Delta_{\text{up}}. \end{aligned} \quad (19)$$

$\Pr(\hat{\eta} \leq \Phi)$ represents the probability that the estimated BLER, given in (18), falls below the threshold Φ . Under stationary channel conditions, $\Pr(\hat{\eta} \leq \Phi)$ can be reasonably approximated by the proportion of high-margin-ACKs $\eta(\Phi)$. The recurrence function for δ_t can be expressed as

$$\begin{aligned} T(\delta) = & \delta + \eta_t \Delta_{\text{up}} - (1 - \eta_t) \eta(\Phi) \Delta_{\text{down}} \\ & + (1 - \eta_t)(1 - \eta(\Phi)) \Delta_{\text{up}}. \end{aligned} \quad (20)$$

As in the proof of **Theorem 1**, the first and second Banach fixed point conditions should be satisfied to guarantee the convergence of BLER. As δ_t becomes increasingly smaller, the SNR estimates rises until the BLER η_t reaches 1. This would lead to the same lower bound discussed in **Theorem 1**. On the other hand, as δ_t increases and the value of η_t gradually drops to 0, the upper bound under soft link adaptation becomes

$$\delta_{\text{max}} - \eta(\Phi)\Delta_{\text{down}} + (1 - \eta(\Phi))\Delta_{\text{up}}. \quad (21)$$

In order to ensure that $T(\delta)$ is a contract mapping, we need to ensure the upper bound is smaller than δ_{max} , that is

$$\begin{aligned} \delta_{\text{max}} - \eta(\Phi)\Delta_{\text{down}} + (1 - \eta(\Phi))\Delta_{\text{up}} & \leq \delta_{\text{max}} \\ \Rightarrow 1 > \eta(\Phi) & \geq \frac{1}{1 + \frac{\Delta_{\text{down}}}{\Delta_{\text{up}}}}. \end{aligned} \quad (22)$$

Proof for the second Banach fixed condition can be found in Appendix B. When t approaches infinity, we have that

$$\lim_{t \rightarrow \infty} \eta_t = \frac{(1 - \frac{1}{\eta(\Phi)}) \frac{\Delta_{\text{up}}}{\Delta_{\text{down}}} + 1}{1 + \frac{\Delta_{\text{up}}}{\Delta_{\text{down}}}} < \frac{1}{1 + \frac{\Delta_{\text{up}}}{\Delta_{\text{down}}}}. \quad (23)$$

□

Compared with (17), the achieved BLER after convergence will be lower than that of OLLA. This analytically justifies the better performance of the proposed soft link adaptation scheme. By introducing BLER estimation, we utilized more channel information beyond raw ACK/NACK indicators for adjusting the channel SNR estimates. Furthermore, this method is simpler and exhibits stronger generalization capabilities than other link adaptation methods based on Bayesian inference or reinforcement learning (RL).

C. MAC: Video-aware Resource Allocation

The MAC layer efficiently employs a scheduler to manage the number of RBs allocated. As previously discussed, both the MCS and RB allocation influence the TB size, thereby affecting the link's throughput. Nevertheless, the MCS is determined by link adaptation, which must meet the BLER constraint. Adopting a more 'aggressive' MCS selection strategy will increase the block size, but it also enlarges the probability of erroneous block decoding, which in turn reduces the overall throughput. In contrast, resource allocation at the MAC layer affects the throughput with a minimal impact on BLER. Thus, optimizing resource allocation at the MAC layer can achieve better bandwidth control. During video streaming, the bitrate ladder shows significant gaps between consecutive blocks. These discontinuities coupled with imprecise throughput prediction result in a severe mismatch between the chunk bitrate and the actual throughput. Current resource allocation does not take into account the impact of throughput mismatches. Based on these considerations, we propose the following video-aware resource allocation that aligns the throughput with the chunk bitrate by acquiring the bitrate information from APP.

As the chunk length (with an order of seconds) is much longer compared to TTI (with an order of milliseconds) for resource allocation, it is challenging for MAC to quickly affect the bitrate decisions at APP. Therefore, we adopt a top-down optimization approach in which resource allocation at the MAC layer during the downloading of a chunk is constrained and guided by chunk bitrate selected by the APP layer. This aims to more closely align throughput the chunk bitrate to maximize rate utilization. Assuming e_{max} resource blocks are available at the base station, we formulate an integer linear programming problem for video-aware resource allocation (VRA), which is

$$\mathbf{P3:} \quad \min_{\{e_t\}_{t=m, 2m, \dots, d_i}} \sum_{i=1}^D \left| \sum_{t=1}^{d_i} N_{\tau_t, e_t} (1 - \eta_{e_t, \gamma_t}) - \rho(a_{i,i}) \right|$$

s.t. Constraints from Eqs. (1), (2), (3), (5), and (6).

At time t when decisions are made (at the start of each TTI), since the BLER η_{e_t, γ_t} is unknown, we utilizes (18) to estimate

BLER $\hat{\eta}_{\gamma_t, \tau_t}$ from past observations. The TB size N_0 that best matches the bitrate of the chunk is calculated as

$$N_0 = \frac{\rho(a_{i,l})}{(1 - \hat{\eta}_{\gamma_t, \tau_t})T_{\text{chunk}}}. \quad (24)$$

However, the number of RBs is an integer, while N_0 takes a positive real value. For practical implementation, we select e_t from the set $\{0, 1, \dots, e_{max}\}$, based on the known MCS τ_t from soft link adaptation, that generates the TB size N_{τ_t, e_t} closest to N_0 . The simplicity of our approach lies in its algorithmic complexity being $O(n)$. While the estimation of N_0 may be rough, as the TTI of resource allocation increases during a single chunk download period, the total throughput tends to approach the bitrate of the downloaded chunk.

D. APP: Adaptive Bitrate

In APP, it is essential to make decisions regarding the chunk bitrate of a video file to optimize the overall QoE:

$$\mathbf{P4:} \quad \max_{\{a_{i,l}\}_{i=1,2,\dots,D}} \sum_{i=1}^D \text{QoE}_i$$

s.t. Constraints from Eqs. (1), (5), (6), and, (8).

We employ the classic ABR strategy, MPC, as our bitrate decision module. Given that MPC employs a rate-based mechanism, it is able to fully leverage the benefits brought by our precise throughput prediction mechanism. Additionally, it combines the forecasted throughput in order to enhance the QoE for several upcoming chunks, demonstrating some extent of resilience. Nonetheless, this does not mean that our platform is not compatible with other ABR algorithms. We will demonstrate at the end of our paper that our cross-layer design brings various levels of enhancement to all current ABRs.

MPC gathers historical chunk throughput to forecast the throughput available for downloading several future chunks. It then conducts playback simulation based on the predicted throughput, selecting the first bitrate from the combination with the highest QoE scores as the decision bitrate for the forthcoming chunk. With the the abundance of timeslots in PHY transmission, the average channel capacities are calculated by measuring them over a set number of timeslots to creating a historical sequence that is uniformly distributed in time (e.g., every 500 slots). These measurements are used with a sliding window to compute the harmonic mean to predict the capacity of the upcoming channel condition. As mentioned previously, a significant advantage of utilizing measurements from PHY is the ability to create uniformly spaced throughput sequences (Fig. 4), thereby removing the irregular time distribution caused by different download durations at chunk level measurement.

E. Summary

This section presents our proposed soft link adaptation at PHY, video-aware resource allocation at MAC, and MPC-S (MPC on StreamOptix) at APP. These mechanisms form a closed loop and reinforce each other. Unfortunately, this work does not extend to multi-user systems, primarily due to

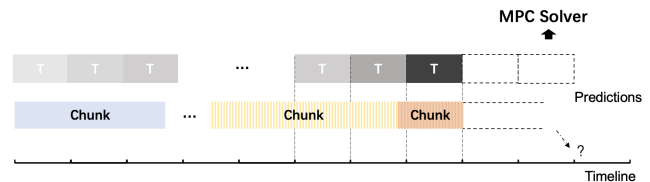


Fig. 4: Uniformly spaced throughput in StreamOptix (upper) v.s. non-uniformly spaced throughput in chunk-level measurement (bottom).

TABLE II: Parameter configuration for wireless link.

Scenario and Configuration Parameter	Value	
Channel Type	TDL C	
Subcarrier Spacing	15 kHz	
Channel Bandwidth	20 MHz	
Resource Grid	0-52	
Maximum HARQ Retransmissions	3	
LDPC Maximum Decoding Iterations	10	
Transport Block Duration	1 ms	
Target BLER	0.1	
Step size Δ_{up}	0.4 dB	
Maximum deviation	3 dB	
Soft-ACK Threshold Φ	0.92	
Throughput Prediction Interval	600ms	
Channel Conditions	SNR	Doppler Shift
Static	-5 - 5 dB	10 Hz
Dynamic	-5 - 5 dB	50 Hz
High SNR	5 - 15 dB	10 Hz

the incompatibility of *MATLAB Simulink*'s custom link-level and system-level simulations. Moreover, multi-user scenarios introduce conflicts between individual optimality and fairness, making it challenging to determine the optimal solution. For completeness, we briefly discuss how StreamOptix can be extended to multi-user cases. For link adaptation, the adjustment needed is to replace SNR estimates with SINR (signal-to-interference and noise ratio) to account for the interference from other users. MAC is a little bit more complicated as it involves fairness among multiple users. Therefore, a two-layer resource allocation strategy can be considered, where the first layer employs the current multi-user resource allocation strategy, like round robin and proportional fairness, while the second layer adopts video-aware resource allocation. The ultimate resource distribution results from multiplying the ratios from both layers element-wise, using trade-off weights. APP does not require any further modification, as it makes bitrate decisions for each user separately.

IV. STREAMOPTIX IMPLEMENTATION

In this section, we describe the implementation of StreamOptix, as well as the extensive evaluation of our proposed cross-layer scheme over numerous metrics. To create StreamOptix, we use *MATLAB* and *Python* to construct the wireless link and video player respectively. We use *matlab.engine* API to enable real-time communication between wireless link deployed in *MATLAB*'s and the virtual player in *Python*. This setup guarantees the separation of higher and lower layer functionalities, enhancing scalability of our platform and enabling future extensions.

TABLE III: Evaluation of different ABRs on static/dynamic/high SNR channel conditions.

Metrics		Static					Dynamic					High SNR				
ABR		FESTIVE	BBA	BOLA	HYB	MPC-S	FESTIVE	BBA	BOLA	HYB	MPC-S	FESTIVE	BBA	BOLA	HYB	MPC-S
PHY	BLER	0.30	0.30	0.32	0.28	0.15	0.397	0.412	0.415	0.32	0.19	0.214	0.273	0.198	0.191	0.067
	BER	0.008	0.004	0.006	0.0006	0.0002	0.014	0.008	0.009	0.012	0.003	0.0013	0.0027	0.0017	0.0006	0.000
VQA	PSNR	30.50	29.52	29.37	27.52	33.01	27.41	27.48	27.56	27.18	32.14	34.64	33.26	33.56	36.09	40.02
	SSIM	0.780	0.801	0.736	0.721	0.86	0.74	0.75	0.77	0.69	0.843	0.88	0.83	0.84	0.91	0.97
APP	Average Bitrate	4.49	4.27	3.99	4.20	4.81	3.84	3.48	3.52	3.84	3.85	4.47	4.14	4.25	4.48	4.99
	Average Rebuffering	0.082	0.053	0.008	0.056	0.018	0.169	0.019	0.014	0.096	0.02	0.072	0.0082	0.019	0.032	0.015
	Average QoE	2.85	3.05	2.16	2.78	4.11	1.47	1.49	1.66	1.74	2.01	2.65	2.74	2.69	3.44	4.63

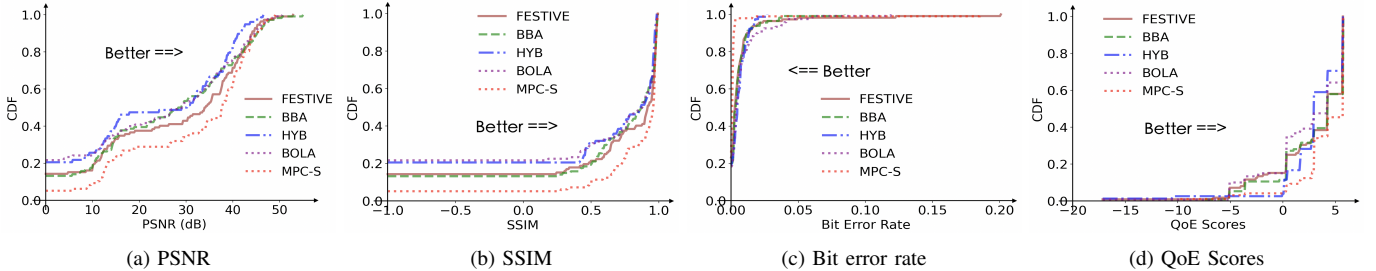


Fig. 5: Evaluation on static link.

TABLE IV: Methods evaluation details, VRA stands for video-aware resource allocation and 3GPP stands for default 3GPP MCS lookup.

Methods	MPC-S	MPC-a	MPC-b	FESTIVE	BOLA	BBA	HYB
APP	MPC	MPC	MPC	FESTIVE	BOLA	BBA	HYB
MAC	VRA	Full grid	Full grid	Full grid	Full grid	Full grid	Full grid
PHY	Soft link adaptation	Soft link adaptation	3GPP	3GPP	3GPP	3GPP	3GPP

A. Simulation Setting

A 5G PDSCH is configured in *Matlab R2022b* to simulate the multipath propagation and Doppler shift of wireless link. Channel type is set as tapped delay line C and LDPC is deployed for channel coding. The SNR is adjusted between -5 dB and 15 dB and the doppler shift is set from 10 to 50Hz to mimic various channel scenarios, specifically static, dynamic, and high SNR. Specifics of the simulation setup are provided in Table II. It is worth noting that our parameter settings for OLLA offset Δ_{up} , Δ_{down} and soft-ACK threshold Φ strictly adhere to our theoretical analysis in Section III.

Methods: For ABRs, we choose four commonly used ABR techniques as baselines. FESTIVE [8], a rate-based approach, predicts throughput based on historical measurements and selects the closest corresponding bitrate. BBA (buffer-based strategy) makes decisions according to the buffer level. HYB (Hybrid) takes both buffer level and throughput prediction into consideration for better trade-off. BOLA employs Lyapunov optimization to derive an optimal buffer-based strategy. MPC-S is our proposed scheme, which is short for MPC on StreamOptix. As current *MATLAB simulink* takes too long for link simulation, our comparison does not include learning-based ABRs, which trains ABR agent offline based on simulation interactions.

To highlight the gain achieved by our cross-layer design, we configure all ABR baseline's link adaptation scheme to the 3GPP default link adaptation scheme and implement resource allocation with a full grid (RB count stays at e_{max} during throughout transmission). MPC-a and MPC-b are ablation versions for MPC-S that sequentially remove soft link adaptation and video-aware resource allocation strategies. Details about method configuration is illustrated in Table IV.

Dataset: We employ the Waterloo Dataset [44] as the streaming source, which comprises twenty videos (including

documentaries, sports, and gaming). These videos, each 10 seconds long, are offered in 11 distinct quality levels ranging from 240p to 1440p, encoded in H.264 format. A bitrate ladder is constructed from these 11 quality levels, set at [750, 1750, 2350, 3000, 4300, 7000] kbps. Each video is segmented into 2-second chunks using *FFmpeg* with a Constant Rate Factor of 23. Every simulation run consists of one hundred video segments, culminating in a total viewing time of 200 seconds.

Evaluation Metrics: To evaluate ABR performance at APP, we analyze the video bitrate, rebuffering, and QoE scores. We compute the PSNR (Peak Signal-to-Noise Ratio) and SSIM (Structural Similarity Index) to assessing the quality of delivered videos. Additionally, we measure the BLER, bit error rate, and rate utilization during video transmission to assess the performance of wireless link. Rate utilization for chunk i is defined as $\frac{t_{i+1}-t_i}{T_{chunk}}$, t_i represents the time to start downloading chunk i . Rate utilization of 1 indicates the perfect match of video bitrate and transmission throughput. A value exceeding 1 suggests underutilization of the available throughput, whereas a value less than 1 indicates overutilization.

In the following sections, we first provide an overall comparison between MPC-S and other baseline methods across three different link conditions. We then analyze the effects of PHY-aware throughput prediction, video-aware resource allocation (VRA) and soft link adaptation separately to illustrate the gain of our cross-layer design. Finally, we verify that our cross-layer design could serve as a plug-in solution which could enhance the performance of any ABR.

B. Results on StreamOptix Streaming

In the following, we evaluate MPC-S with other baseline methods across three different link environments: static, dynamic, and high SNR (configured according to Table II). The cumulative distribution function (CDF) of SSIM, PSNR, bit error rate and QoE are illustrated in Fig. 5, 6 and 7. Extensive measurements of all metrics are listed in Table III.

Static Scenario: As shown in Fig. 5, MPC-S achieves a significant improvement in objective quality assessments (PSNR, SSIM) compared to other baselines. The improvement is attributed to our soft link adaptation, as confirmed by the bit

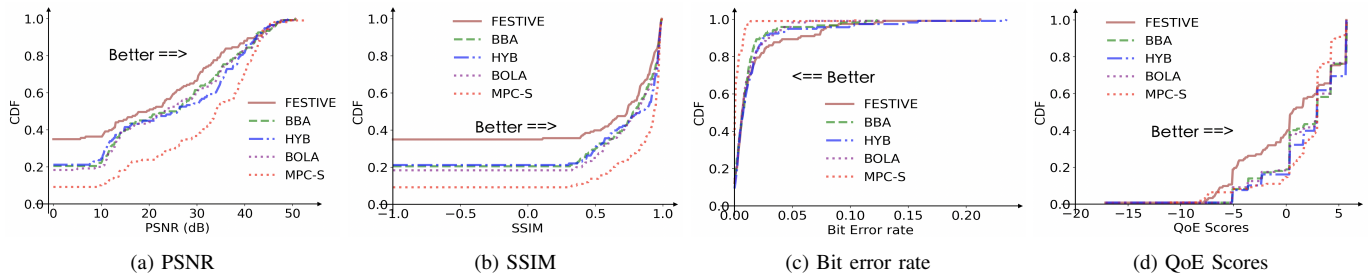


Fig. 6: Evaluation on dynamic link.

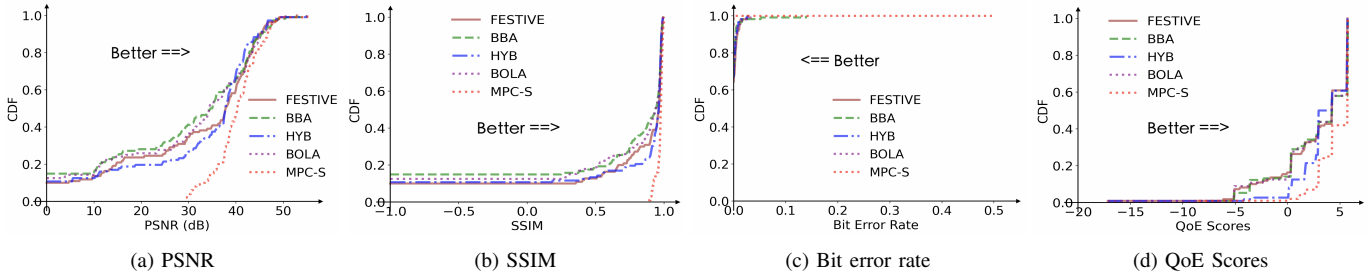


Fig. 7: Evaluation on High SNR link.

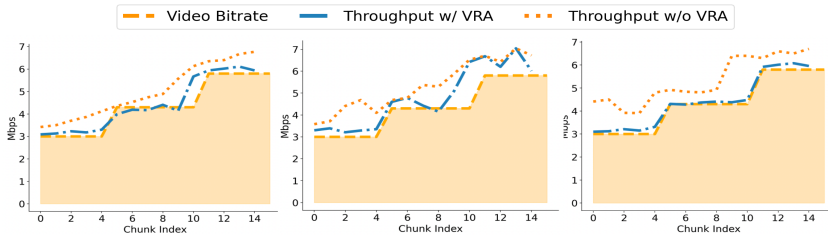


Fig. 8: Chunk bitrate v.s. throughput on Static/Dynamic/High SNR.

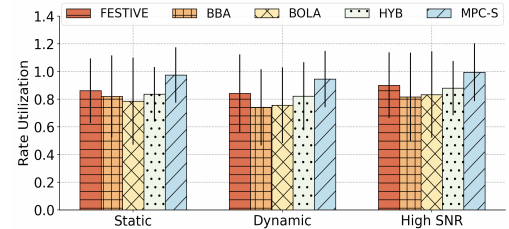


Fig. 9: Evaluation on rate utilization.

rate error curve. Specifically, the intersections at y-axis for the SSIM and PSNR curves suggest the ratio of video decoding failures. This occurs when the essential metadata needed for decoding is corrupted during the transmission of the link. Remarkably, the MPC-S approach shows the lowest occurrence of decoding errors, around 0.05, subtly emphasizing the decrease in errors due to soft link adaptation. In contrast, HYB and BOLA show error rates as high as 20%. The elimination of error rate can be attributed to the incorporation of our soft link adaptation, which enhances the adaptability of link transmission to prevailing channel conditions.

Dynamic Scenario: In dynamic link, the frequent link variations lead to greater variations in throughput. According to Fig. 6, the SSIM and PSNR curves show nearly a twofold rise in the bit error rate across all methods. Results in Table III demonstrate that the MPC-S improves QoE by 14% relative to HYB, which is the most effective among all baselines. SSIM and PSNR of MPC-S reaches 0.843 and 32.14 dB, respectively.

High SNR: The high SNR link simulates the good channel condition with large throughput and small variations. In this case, the increase of SNR leads to a greater link capacity, resulting in improved performance across all methods. As observed in Fig. 7, MPC-S has completely eradicated video decoding errors, significantly enhancing the objective video quality, with PSNR achieving 40.02 dB and SSIM attaining 0.97. Despite the improvement in performance across all methods, MPC-S continues to show superior performance in nearly all metrics. According to Table III, MPC-S outperforms

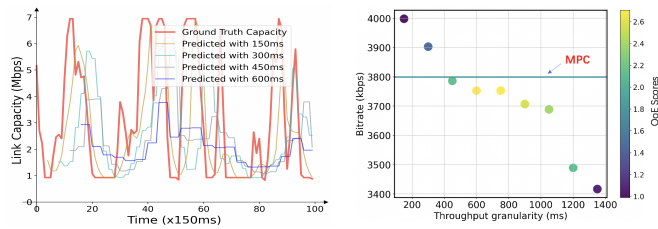
the runner-up method with a 34% enhancement in QoE, an 11% improvement in PSNR, and an 8% rise in SSIM.

Rate Utilization: Fig. 9 exhibits rate utilization of all methods. The results reveal that MPC-S has effectively managed the resource to maximize rate utilization, with recorded values of 0.95, 0.92, and 0.99. In contrast, other methods exhibit a 15%-20% shortfall due to the lack of video bitrate allocation. MPC-S also shows the smallest variance when compared to other methods. To visualize the effects of video-aware resource allocation (VRA), we construct a video bitrate trace with five chunks at rates of 3000kbps, 4300kbps, and 5800kbps. We adjust the SNR of wireless link to ensure that the link capacity marginally exceeds the bitrate in the constructed trace. Fig. 8 illustrates the throughput measurements for each chunk, both with and without VRA implementation. The results indicate improved rate utilization when VRA is applied. Channel throughput demonstrates enhanced stability in both static and elevated SNR scenarios. Given that VRA is influenced by BLER prediction (Eq. (24)), the variance in dynamic link conditions increases as BLER becomes more unpredictable.

V. ANALYSIS AND ABLATION STUDY

A. PHY-aware Throughput Prediction

As previously mentioned, our cross-layer scheme provides regularly sampled link capacities at PHY, which allows for more accurate predictions. Fig. 10a shows the impact of regularly sampled throughput prediction at different granularities. It is evident from the illustration that as the granularity



(a) Predict link capacities with different prediction intervals (b) MPCs with different prediction intervals

Fig. 10: Evaluation on PHY-aware throughput prediction.

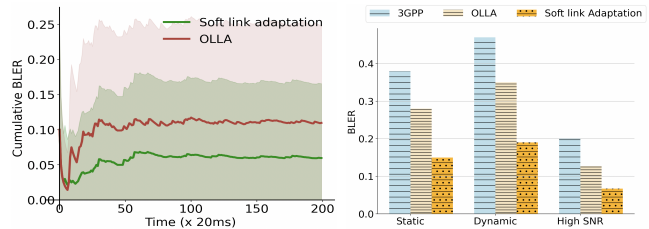
TABLE V: Performance of MPCs on different prediction granularities.

Granularity (ms)	150	300	450	600	750	900
MSE Loss on prediction	3.17	6.94	5.98	3.61	5.20	4.86
QoE Scores	0.99	1.47	2.13	2.70	2.58	2.44
Bitrate (Mbps)	3.998	3.903	3.789	3.753	3.707	3.689
Rebuffer (s)	0.205	0.122	0.058	0.017	0.04	0.059

decreases, the predicted throughput becomes increasingly conservative. Conversely, finer granularities may lead to higher overhead and more aggressive predictions. To determine the optimal prediction granularity that trade off these effects, we assess MPC’s performance using granularities ranging from 150ms to 900ms. Throughput is predicted using harmonic mean of past 8 samples [6]. The results presented in Table V and Fig. 10b indicate that with increasing granularity, the MPC’s average bitrate consistently drops, likely due to more conservative predictions. At finer granularities, the bitrates are notably high, leading to significant rebuffering to deteriorate QoE. With coarser granularities, there is a bitrate reduction accompanied by less rebuffering, which helps mitigate the impact of lower bitrates. An optimal QoE is achieved at a granularity of approximately 600ms. After this threshold, additional reductions in rebuffering do not offset the decline in bitrate. Therefore, we set the granularity of throughput prediction as 600ms throughout our study. In Fig. 10b, the horizontal line depicts the performance of naive MPC [6], which predicts future throughput at chunk level. The results indicate naive MPC’s QoE is approximately 30% worse compared to that of MPC with 600ms prediction granularity.

B. Soft Link Adaptation

As shown in Fig. 11a, soft link adaptation has effectively achieved BLER convergence at chunk level, which reaches stability at around 1 second. This confirms the chunk-level convergence as discussed in Section III B of our theoretical analysis. To demonstrate the average BLER level achieved by soft link adaptation, we assess the average BLER of soft link adaptation, OLLA, and the default 3GPP MCS lookup (3GPP) under different SNR conditions. As illustrated in Fig. 11b, soft link adaptation surpasses the other two schemes, attaining an almost 50% reduction in BLER level across all link conditions. Table VI presents a comprehensive analysis of BLER at two different BLER targets. The results indicate that the BLER convergence is reached at around 5dB SNR under soft link adaptation, significantly lower than the other



(a) Visualization on soft link adaptation convergence (b) BLERs assessed at different link conditions

Fig. 11: Evaluation on soft link adaptation.

TABLE VI: Comparison of BLER performance at different SNR levels.

BLER target	Schemes	SNR					
		-5 dB	0 dB	5 dB	10 dB	15 dB	20 dB
0.1	3GPP	0.7	0.57	0.23	0.05	0.02	0.007
	OLLA	0.54	0.18	0.11	0.03	0.009	0.006
	Soft Link Adaptation	0.55	0.17	0.07	0.02	0.005	0.004
0.05	3GPP	0.7	0.57	0.23	0.05	0.02	0.007
	OLLA	0.54	0.18	0.07	0.02	0.007	0.005
	Soft Link Adaptation	0.55	0.17	0.052	0.015	0.003	0.0014

two. Extensive assessments indicate that soft link adaptation outperforms the other two methods, leading to a more uniform BLER level. This consistency ensures more stable throughput and reduce the bit error rate, ultimately enhancing the quality of the delivered videos.

C. Incremental Ablation Study

To delve deeper into the benefits of soft link adaptation and video aware resource allocation, we conduct an incremental ablation analysis on MPC³. In this analysis, MPC-b denotes the variant lacking both soft link adaptation and video aware resource allocation, whereas MPC-a includes only soft link adaptation. As shown in Fig. 12, the average bit error rate significantly drops from 0.4 to below 0.2 with the implementation of soft link adaptation. Moreover, the addition of VRA to the soft link adaptation leads to a further reduction in the bit error rate, which falls from an average of 0.05 to nearly zero. The rate utilization of MPC is significantly improved by VRA, with MPC-S reaching a mean value of 0.95, compared to 0.8 for MPC-a and 0.75 for MPC-b (Fig. 12e). Additionally, MPC-S exhibits significant improvements in terms of PSNR, SSIM, and QoE.

VI. DISCUSSION AND CHALLENGE

In this study, we present the closed-loop cross-layer optimization platform that integrates interactions across the PHY, MAC, and APP layers. Utilizing our cross-layer transmission framework, any ABR can adopt soft link adaptation and VRA.

Benefits of StreamOptix: To demonstrate the efficacy of our cross-layer design for all ABRs, we have included each ABR with soft link adaptation and VRA in our study for comprehensive assessment. The findings are depicted in Fig. 13a-e. The horizontal axis depicts the metrics evaluated using

³The experimental setup for ablation study is based on the dynamic configuration.

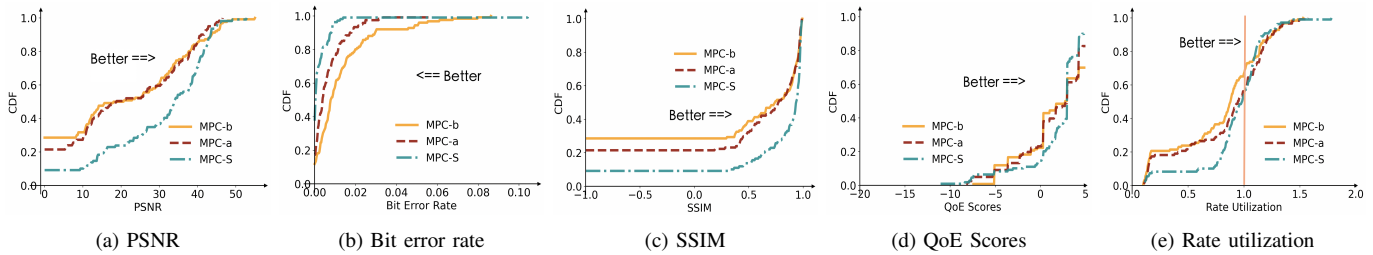


Fig. 12: Ablation study of cross-layer design.

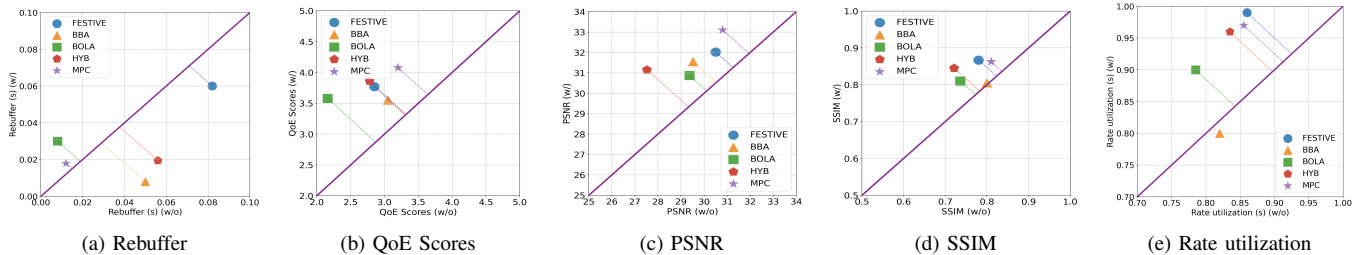


Fig. 13: Benefits of our cross-layer design on different ABRs.

ABRs that include both soft link adaptation and VRA, whereas the vertical axis depicts the metrics assessed using ABRs lacking both cross-layer designs. Thus, the divergence from the diagonal line visually indicates the advantages gained from the cross-layer design. It is evident that, with the exception of BBA, which exhibits no notable variation in SSIM, all metrics show improvements across different ABRs, especially HYB. MPC outperforms all other ABRs in each scenario, validating our selection of MPC as the ABR. StreamOptix is also capable of simulating a range of distortions that replicate real-world transmission situations. Visualizations of these distortions can be found in Appendix C. StreamOptix offers access to both the distorted video bitstreams and the decoded videos. This assists future researchers in collecting additional distorted transmission streams to further explore the impact of various transmission configurations on video quality.

System Complexity: A major hurdle in evaluating StreamOptix is its computational complexity. The transmission of each TB involves channel convolution to account for multipath effects and doppler shift variations, causing a 2-second video chunk simulation to take several minutes. The entire assessment is performed on an Intel i9 processor, requiring approximately one and a half months to complete, thereby constraining the extension of learning-driven ABRs on this system. Future studies will explore the distribution of bit error patterns in simulated video streams across our wireless links. This exploration will help pinpoint distortion patterns within this distribution, enhancing our ability to simulate impairments more accurately in video stream transmission and possibly increasing the efficiency of link simulations. Although our design focuses on a single-user scenario, future research could examine multi-user case by integrating video-aware resource allocation with the existing strategies for multi-user resource allocation as noted in Section III E.

VII. CONCLUSION

In this paper, we proposed a cross-layer video delivery scheme, StreamOptix, to effectively optimize video delivery.

Our proposed three-level closed-loop framework optimizes video delivery across PHY, MAC and APP. In PHY, we propose soft link adaptation that implements soft-ACK feedback to improve the robustness of link adaptation. In MAC, resource allocation is further improved by assigning resource blocks under bitrate constraint to ensure maximum rate utilization. Then, in APP, we redesigned the MPC algorithm for ABR by utilizing link capacities measured from PHY to improve bitrate decision accuracy. Extensive assessments across diverse network conditions reveal substantial improvements of our design in both subjective and objective quality metrics. Furthermore, StreamOptix provides access to distorted transmission streams, enabling a more thorough quality evaluation and supplying multi-modal data for enhanced optimization.

APPENDIX

A. OLLA

According to [40], the second Banach fixed point theorem asserts that the magnitude of the derivative of the recurrence function must be less than 1, that is:

$$|T'(\delta)| < 1, \forall \delta \in [\delta_{\min}, \delta_{\max}]. \quad (25)$$

Recall that the recurrence function for OLLA offset δ_t is

$$T(\delta) = \delta + \eta_t \Delta_{\text{up}} - (1 - \eta_t) \Delta_{\text{down}}. \quad (26)$$

If we treat the average BLER as a function of δ , then we have

$$T'(\delta) = 1 + (\Delta_{\text{up}} + \Delta_{\text{down}}) \cdot \eta'_t(\delta). \quad (27)$$

Note that the average BLER η_t shows a negative correlation with δ . This is because a higher δ can lead to an overestimated SNR, thereby increasing the chance of block decoding errors. According to [37], η_t can be fitted via offline link simulations as $\eta_t(\delta) = 1/(1 + e^{-\alpha_0 \delta - \alpha_1})^s$, where α_0 , α_1 and s are fitting parameters and s controls the slope. In order to satisfy the

Algorithm 1 Soft Link Adaptation Algorithm

Initialize: MCS – Table : $\gamma \rightarrow \tau_{1,2,\dots,15}$; Soft-ACK threshold Φ
Initialize: $\delta_t = \delta_0$, Δ_{down} , Δ_{up} (Specify initial values)
Input: Estimated SNR γ_t from CSI; HARQ feedback flag from UE
for each transmission t **do**
 $\gamma_t = \gamma_t - \delta_t$
 select τ_t from $\gamma \rightarrow \tau_{1,2,\dots,15}$ based on γ_t
 if flag = ACK **then**
 estimate the block error probability $\hat{\eta}_t$
 if $\hat{\eta}_t \leq \Phi$ **then**
 flag = HIGHACK
 else
 flag = LOWACK
 end if
 end if
 if flag = HIGHACK **then**
 $\delta_t \leftarrow \delta_t - \Delta_{\text{down}}$
 else if flag = LOWACK **or** flag = NACK **then**
 $\delta_t \leftarrow \delta_t + \Delta_{\text{up}}$
 end if
end for

second Banach fixed point condition in Eq. (25), since the derivative of $\eta_t(\delta)$ is negative, we have that

$$\begin{aligned}
 (\Delta_{\text{up}} + \Delta_{\text{down}}) \cdot |\eta'_t(\delta)| &< 2 \\
 \Rightarrow |\eta'_t(\delta)| &< \frac{2}{(\Delta_{\text{up}} + \Delta_{\text{down}})}. \quad (28)
 \end{aligned}$$

We are going to find the maximum of $\eta'_t(\delta)$, i.e., the values for which $\eta''_t(\delta) = 0$, to ensure that the second Banach fixed point condition in Eq. (25) is fulfilled. It can be shown that the maximum value of $\eta'_t(\delta)$ can be achieved when the offset δ takes a value equal to

$$\delta_0 = \frac{1}{\alpha_1} \cdot \left(\ln \left(\frac{1}{s} + \alpha_0 \right) \right). \quad (29)$$

Therefore, the maximum value of $|\eta'_t(\delta)|$ is

$$|\eta'_t(\delta)| = |\alpha_1| \cdot \frac{1}{(1 + 1/s)^{s+1}}. \quad (30)$$

An upper bound on $\eta'_t(\delta)$ can thus be found by setting $s \rightarrow \infty$, which is

$$|\eta'_t(\delta)| = \frac{|\alpha_1|}{e}. \quad (31)$$

According to [37], α_1 is set to be -1.11, Combining (28) and (31) yields

$$\Delta_{\text{down}} + \Delta_{\text{up}} \leq \frac{2e}{1.11}. \quad (32)$$

Therefore, convergence is guaranteed if $\Delta_{\text{up}} + \Delta_{\text{down}}$ does not exceed a certain limit $\frac{2e}{1.11}$.

B. Soft link adaptation

Recall that the recurrence function for soft link adaptation is

$$\begin{aligned}
 T(\delta) &= \delta + \eta_t \Delta_{\text{up}} - (1 - \eta_t) \eta(\Phi) \Delta_{\text{down}} \\
 &\quad + (1 - \eta_t)(1 - \eta(\Phi)) \Delta_{\text{up}}. \quad (33)
 \end{aligned}$$

Similarly, by taking the derivative of both sides, we have

$$T'(\delta) = 1 + (\eta(\Phi)(\Delta_{\text{up}} + \Delta_{\text{down}})) \cdot \eta'_t(\delta). \quad (34)$$

Since $\eta(\Phi) \leq 1$, in order to satisfy second Banach fixed point condition in Eq. (1), we have

$$|\eta'_t(\delta)| < \frac{2}{\eta(\Phi)(\Delta_{\text{down}} + \Delta_{\text{up}})}. \quad (35)$$

In the main text, it has been shown that the requirement for the first Banach fixed point condition to be satisfied by the soft link adaptation is

$$\eta(\Phi) \geq \frac{1}{1 + \frac{\Delta_{\text{down}}}{\Delta_{\text{up}}}}. \quad (36)$$

Referring to Eq. (31), which establishes the maximum value of $\eta'_t(\delta)$ as $|\alpha_1|/e$, and combining Eq. (11) and (12), the parameters Δ_{down} and Δ_{up} must fulfill

$$\Delta_{\text{up}} \leq \frac{2e}{1.11}. \quad (37)$$

Therefore, convergence is guaranteed if Δ_{up} does not exceed $\frac{2e}{1.11}$.

Algorithm 2 Video adaptation flow on MPC-S

Initialize: Prediction window length M ; Throughput prediction interval T ; Video file length D ; History window length N ;
for $k = 1$ to D **do**

$$\hat{C}_{[t_k, \dots, t_k + M * T]} = \text{ThroughputPred}(C_{[t_k - N * T, \dots, t_k]})$$

$$\text{QoE}_{max} = 0$$

for each possible M -length bitrate trace $a_{[k, \dots, k + M - 1]}$ **do**

$$\text{QoE}_{[k, \dots, k + M - 1]} = 0$$

for $i = 1$ to M **do**

$$d_i = 0; \text{acc_size} = 0$$

Calculate the transmission delay d_i :

for $j = 0$ **do**

if $\text{acc_size} + \hat{C}_{t_k + j * T} * T \geq \rho(a_i)$ **then**

$$d_i += \frac{\rho(a_i) - \text{acc_size}}{\hat{C}_{t_k + j * T}}$$

Break

end if

$$d_i += T; \text{acc_size} += \hat{C}_{t_k + j * T} * T; j += 1$$

end for

Calculate rebuffering: $\phi_i = (d_i - b_i)_+$

Calculate QoE: $\text{QoE}_i = a_{i,l} - \alpha |a_{i,l} - a_{i-1,l}| - \beta \phi_i$

Update timeline: $t_{i+1} = t_i + d_i$

Update buffer occupancy: $b_{i+1} = (b_i - d_i) + T_{\text{chunk}}$

end for

$$\text{QoE}_{[k, \dots, k + M - 1]} += \text{QoE}_i$$

if $\text{QoE}_{[k, \dots, k + M - 1]} \geq \text{QoE}_{max}$ **then**

$$\text{QoE}_{max} = \text{QoE}_{[k, \dots, k + M - 1]}$$

end if

end for

Output the first element a_{k+1} from the bitrate trace that achieves the maximum $\text{QoE}_{[k, \dots, k + M - 1]}$

end for



Fig. 14: Visualization of the distortion patterns captured in StreamOptix.

C. Visualization of video distortions

Fig. 14 shows different distortions captured when transmitting videos over StreamOptix. In particular, once the video stream is encoded into a bitstream at the application layer, it is then encapsulated into transport blocks (TBs) when it reaches the wireless link. These TBs are subject to random

multipath fading and doppler spread within the wireless link, which can hinder their correct decoding at the receiver's end. As a result, this can impact the bitstream decoding process, causing various types of video distortion. Compared with existing trace-driven based ABR emulation platforms (Pensieve), StreamOptix is able to simulate various realistic corruption patterns including reference error (a, b), misalignment (c, d), color artifacts (e, f), block artifacts (g, h), texture loss (i, j), duplication artifacts (k, l). These distortion patterns are influenced not only by the bit error rate of the transmitted video but also by the error location, which tends to be random and unpredictable. Therefore, the most effective way to mitigate these issues is to enhance PHY link adaptation to lower the likelihood of errors. In the future, we could integrate error-specific video recovery methods into our system for further enhancements. As shown in Fig. 1, videos transmitted via StreamOptix more closely resemble corrupted videos in real-world scenarios.

REFERENCES

- [1] M. Liu, J. Chen, G. Wu, L. Ji, and H. Wang, "Soft-ack based outer loop link adaptation for latency-constrained 5g video conferencing," in *GLOBECOM 2023 - 2023 IEEE Global Communications Conference*, 2023, pp. 388–393.
- [2] "Ericsson's annual report 2022," <https://www.ericsson.com/en/investors/financial-reports/order-annual-report>, 2022.
- [3] "ISO/IEC 23009-1:2022. Information technology — Dynamic adaptive streaming over HTTP (DASH) — Part 1: Media presentation description and segment formats," ISO/IEC, Standard, Aug. 2022.
- [4] Z. Lu and G. de Veciana, "Optimizing stored video delivery for wireless networks: The value of knowing the future," *IEEE Transactions on Multimedia*, vol. 21, no. 1, pp. 197–210, 2019.
- [5] K. Spiteri, R. Ugaonkar, and R. K. Sitaraman, "Bola: Near-optimal bitrate adaptation for online videos," *IEEE INFOCOM 2016 - The 35th Annual IEEE International Conference on Computer Communications*, pp. 1–9, 2016.
- [6] X. Yin, A. Jindal, V. Sekar, and B. Sinopoli, "A control-theoretic approach for dynamic adaptive video streaming over http," *Proceedings of the 2015 ACM Conference on Special Interest Group on Data Communication*, 2015.
- [7] H. Mao, R. Netravali, and M. Alizadeh, "Neural adaptive video streaming with pensieve," *Proceedings of the Conference of the ACM Special Interest Group on Data Communication*, 2017.
- [8] J. Jiang, V. Sekar, and H. Zhang, "Improving fairness, efficiency, and stability in http-based adaptive video streaming with festive," *IEEE/ACM Transactions on Networking*, vol. 22, no. 1, pp. 326–340, 2014.
- [9] J. Pei, C. An, A. Zhou, L. Liu, and H. Ma, "Par: Improving video bitrate adaptation via payload-aware throughput prediction," in *2022 IEEE International Conference on Multimedia and Expo (ICME)*, 2022, pp. 1–6.
- [10] F. Y. Yan, H. Ayers, C. Zhu, S. Fouladi, J. Hong, K. Zhang, P. Levis, and K. Winstein, "Learning in situ: a randomized experiment in video streaming," in *17th USENIX Symposium on Networked Systems Design and Implementation (NSDI 20)*. Santa Clara, CA: USENIX Association, Feb. 2020, pp. 495–511. [Online]. Available: <https://www.usenix.org/conference/nsdi20/presentation/yan>
- [11] H. Saki and M. Shikh-Bahaei, "Cross-layer resource allocation for video streaming over ofdma cognitive radio networks," *IEEE Transactions on Multimedia*, vol. 17, no. 3, pp. 333–345, 2015.
- [12] Y. F. Yeznabad, M. Helfert, and G.-M. Muntean, "Cross-layer joint optimization algorithm for adaptive video streaming in mec-enabled wireless networks," in *2021 IEEE International Symposium on Broadband Multimedia Systems and Broadcasting (BMSB)*, 2021, pp. 1–6.
- [13] Z. Yan, J. Xue, and C. W. Chen, "Prius: Hybrid edge cloud and client adaptation for http adaptive streaming in cellular networks," *IEEE Transactions on Circuits and Systems for Video Technology*, vol. 27, no. 1, pp. 209–222, 2017.
- [14] M. Kim and K. Chung, "Edge computing assisted adaptive streaming scheme for mobile networks," *IEEE Access*, vol. 9, pp. 2142–2152, 2021.

- [15] Y. F. Yeznabad, M. Helffert, and G.-M. Muntean, "Backhaul traffic and qoe joint optimization approach for adaptive video streaming in mecenabled wireless networks," in *2022 IEEE International Symposium on Broadband Multimedia Systems and Broadcasting (BMSB)*, 2022, pp. 1–6.
- [16] K. Tang, N. Kan, J. Zou, C. Li, X. Fu, M. Hong, and H. Xiong, "Multi-user adaptive video delivery over wireless networks: A physical layer resource-aware deep reinforcement learning approach," *IEEE Transactions on Circuits and Systems for Video Technology*, vol. 31, no. 2, pp. 798–815, 2021.
- [17] 3GPP, "Evolved Universal Terrestrial Radio Access (E-UTRA) and Evolved Universal Terrestrial Radio Access Network (E-UTRAN)," 3GPP, Technical Report TS 36.300 Rel. 11, Sep. 2012. [Online]. Available: https://www.etsi.org/deliver/etsi_ts/136300_136399/136300/11.03.00_60/ts_136300v110300p.pdf
- [18] M. G. Sarret, D. Catania, F. Frederiksen, A. F. Cattoni, G. Berardinelli, and P. Mogensen, "Dynamic outer loop link adaptation for the 5g centimeter-wave concept," in *Proceedings of European Wireless 2015; 21th European Wireless Conference*, 2015, pp. 1–6.
- [19] J. Fan, Q. Yin, G. Y. Li, B. Peng, and X. Zhu, "MCS selection for throughput improvement in downlink LTE systems," in *2011 Proceedings of 20th International Conference on Computer Communications and Networks (ICCCN)*, 2011, pp. 1–5, doi: 10.1109/ICCCN.2011.6005743.
- [20] E. Peralta, G. Pocovi, L. Kuru, K. Jayasinghe, and M. Valkama, "Outer loop link adaptation enhancements for ultra reliable low latency communications in 5G," in *2022 IEEE 95th Vehicular Technology Conference: (VTC2022-Spring)*, 2022, pp. 1–7, doi: 10.1109/VTC2022-Spring54318.2022.9860717.
- [21] V. Saxena and J. Jaldén, "Bayesian link adaptation under a BLER target," in *2020 IEEE 21st International Workshop on Signal Processing Advances in Wireless Communications (SPAWC)*, 2020, pp. 1–5, doi: 10.1109/SPAWC48557.2020.9154253.
- [22] M. Li, Z. Chen, and Y.-P. Tan, "A maxmin resource allocation approach for scalable video delivery over multiuser mimo-ofdm systems," in *2011 IEEE International Symposium of Circuits and Systems (ISCAS)*, 2011, pp. 2645–2648.
- [23] L. Tong, Y. Chen, X. Zhou, and Y. Sun, "Qoe-fairness tradeoff scheme for dynamic spectrum allocation based on deep reinforcement learning," in *Proceedings of the 5th International Conference on Computer Science and Application Engineering*, ser. CSAE '21. New York, NY, USA: Association for Computing Machinery, 2021. [Online]. Available: <https://doi.org/10.1145/3487075.3487137>
- [24] Z. Akhtar, Y. S. Nam, R. Govindan, S. Rao, J. Chen, E. Katz-Bassett, B. Ribeiro, J. Zhan, and H. Zhang, "Oboe: Auto-tuning video abr algorithms to network conditions," in *Proceedings of the 2018 Conference of the ACM Special Interest Group on Data Communication*, ser. SIGCOMM '18. Association for Computing Machinery, 2018, p. 44–58.
- [25] Y. Sun, X. Yin, J. Jiang, V. Sekar, F. Lin, N. Wang, T. Liu, and B. Sinopoli, "Cs2p: Improving video bitrate selection and adaptation with data-driven throughput prediction," in *Proceedings of the 2016 ACM SIGCOMM Conference*, ser. SIGCOMM '16. New York, NY, USA: Association for Computing Machinery, 2016, p. 272–285.
- [26] H. T. Le, D. V. Nguyen, N. P. Ngoc, A. T. Pham, and T. C. Thang, "Buffer-based bitrate adaptation for adaptive http streaming," in *2013 International Conference on Advanced Technologies for Communications (ATC 2013)*, 2013, pp. 33–38.
- [27] T. Huang, C. Zhou, R.-X. Zhang, C. Wu, X. Yao, and L. Sun, "Comyco: Quality-aware adaptive video streaming via imitation learning," in *Proceedings of the 27th ACM International Conference on Multimedia*, ser. MM '19. New York, NY, USA: Association for Computing Machinery, 2019, p. 429–437. [Online]. Available: <https://doi.org/10.1145/3343031.3351014>
- [28] T. Huang, R.-X. Zhang, and L. Sun, "Zwei: A self-play reinforcement learning framework for video transmission services," *IEEE Transactions on Multimedia*, vol. 24, pp. 1350–1365, 2022.
- [29] Y. Li, H. Chen, B. Xu, Z. Zhang, and Z. Ma, "Improving adaptive real-time video communication via cross-layer optimization," *IEEE Transactions on Multimedia*, vol. 26, pp. 5369–5382, 2024.
- [30] F. Shamiéh and X. Wang, "Dynamic cross-layer signaling exchange for real-time and on-demand multimedia streams," *IEEE Transactions on Multimedia*, vol. 21, no. 8, pp. 1893–1904, 2019.
- [31] Y.-J. Yu, A.-C. Pang, and M.-Y. Yeh, "Video encoding adaptation for qoe maximization over 5g cellular networks," *Journal of Network and Computer Applications*, vol. 114, pp. 98–107, 2018. [Online]. Available: <https://www.sciencedirect.com/science/article/pii/S1084804518301346>
- [32] G. Xiong, X. Qin, B. Li, R. Singh, and J. Li, "Index-aware reinforcement learning for adaptive video streaming at the wireless edge," in *Proceedings of the Twenty-Third International Symposium on Theory, Algorithmic Foundations, and Protocol Design for Mobile Networks and Mobile Computing*, ser. MobiHoc '22. New York, NY, USA: Association for Computing Machinery, 2022, p. 81–90.
- [33] G. Pan, S. Xu, S. Zhang, X. Chen, and Y. Sun, "Quality of experience oriented cross-layer optimization for real-time xr video transmission," *IEEE Transactions on Circuits and Systems for Video Technology*, pp. 1–1, 2024.
- [34] Y.-H. Jung, Q. Song, K.-H. Kim, P. Cosman, and L. B. Milstein, "Cross-layer resource allocation using video slice header information for wireless transmission over lte," *IEEE Transactions on Circuits and Systems for Video Technology*, vol. 28, no. 8, pp. 2024–2037, 2018.
- [35] X. Xie, X. Zhang, S. Kumar, and L. E. Li, "pistream: Physical layer informed adaptive video streaming over lte," in *Proceedings of the 21st Annual International Conference on Mobile Computing and Networking*, ser. MobiCom '15. New York, NY, USA: Association for Computing Machinery, 2015, p. 413–425. [Online]. Available: <https://doi.org/10.1145/2789168.2790118>
- [36] K. Xiao, S. Mao, and J. K. Tugnait, "Robust qoe-driven dash over ofdma networks," *IEEE Transactions on Multimedia*, vol. 22, no. 2, pp. 474–486, 2020.
- [37] F. Blaquez-Casado, G. Gómez, M. C. Aguayo-Torres, and J. T. Entrambasaguas, "eolla: an enhanced outer loop link adaptation for cellular networks," *EURASIP Journal on Wireless Communications and Networking*, no. 20, 2016.
- [38] R. Giuliano and F. Mazzenga, "Exponential effective sinr approximations for ofdm/ofdma-based cellular system planning," *IEEE Transactions on Wireless Communications*, vol. 8, no. 9, pp. 4434–4439, Sep 2009.
- [39] C. E. Shannon, "A mathematical theory of communication," *ACM SIGMOBILE Mobile Computing and Communications Review*, vol. 5, no. 1, pp. 3–55, 2001.
- [40] S. Banach, "Sur les operations dans les ensembles abstraits et leur application aux equations integrales," Ph.D. dissertation, University of Lwow, Poland (now Ukraine), 1920.
- [41] J. G. Nemeth, M. Al-Imari, and W. Ozan, "Soft-ACK feedback based link adaptation for latency critical applications in 5G/B5G," in *2021 IEEE Global Communications Conference (GLOBECOM)*, 2021, pp. 01–06, doi: 10.1109/GLOBECOM46510.2021.9685435.
- [42] J. G. Nemeth, M. Al-Imari, and W. Ozan, "Soft-ack feedback based link adaptation for latency critical applications in 5g/b5g," in *2021 IEEE Global Communications Conference (GLOBECOM)*, 2021, pp. 01–06.
- [43] R.-H. Hwang, C.-Y. Wang, J.-N. Hwang, Y.-R. Lin, and W.-Y. Chen, "Optimizing live layered video multicasting over LTE with mobile edge computing," *IEEE Transactions on Vehicular Technology*, vol. 69, no. 10, pp. 12 072–12 084, 2020, doi: 10.1109/TVT.2020.3011633.
- [44] Z. Duanmu, A. Rehman, and Z. Wang, "A quality-of-experience database for adaptive video streaming," *IEEE Transactions on Broadcasting*, vol. 64, no. 2, pp. 474–487, 2018, doi:10.1109/TBC.2018.2822870.